Progress In Electromagnetics Research, PIER 104, 385–401, 2010

ELECTROMAGNETIC SCATTERING BY CONDUCTING BOR COATED WITH CHIRAL MEDIA ABOVE A LOSSY HALF-SPACE

D. Z. Ding and R. S. Chen

Department of Communication Engineering
Nanjing University of Science and Technology
Nanjing 210094, China

Abstract—Electromagnetic scattering by conducting bodies of revolution (BOR) coated with homogeneous chiral media above a lossy half-space is formulated in terms of the Poggio-Miller-Chang-Harrington-Wu surface integral equation combined with combined field integral equation. A field decomposition scheme is utilized to split a chiral media into two equivalent homogeneous media. The spatial domain half-space Green's functions are obtained via the discrete complex image method. Due to the rotational symmetry property of BOR, the method of moment for BOR (BORMoM) is applied to the linear system solved by the multifrontal direct solver. Numerical results are presented to demonstrate the accuracy and efficiency of the proposed method.

1. INTRODUCTION

Electromagnetic scattering of novel chiral materials has drawn considerable attention in recent years [1–4]. Progress in the construction of artificial chiral media could possibly result in the production of microwave components with new properties. Since the chirality parameter provides an extra degree of freedom, it may be possible to use chiral materials to coat an object to achieve more effective control of its scattering properties [4]. There have been a lot of efforts made to develop an efficient numerical technique to solve the electromagnetic scattering problems associated with chiral objects, for example the eigenfunction solutions [5–7], volume formulation [8–10], T-matrix method [11–13], and method of moment (MoM) solution [14, 15], finite element method (FEM) [16] as well

Corresponding author: D. Ding (dzding@mail.njust.edu.cn).

as finite difference time domain (FDTD) techniques [17–19]. More recently, surface integral equation (SIE) analysis of homogenous chiral object has been presented in [20–22] with the MoM solution accelerated by Multilevel fast multipole method (MLFMM) [23, 24]. The SIE is also applied to analyze scattering from a homogeneous chiral body solved by MoM for body of revolution (BORMoM) [15]. This work presents an extension of SIE for the efficient analysis of electromagnetic scattering by conducting bodies of revolution (BOR) coated with chiral media located above a lossy half-space.

The problem of electromagnetic scattering from conducting BOR coated with chiral media above a lossy half-space is formulated using the Poggio-Miller-Chang-Harrington-Wu integral equation combined with combined field integral equation (PMCHW-CFIE) [25–27]. The discrete complex-image method (DCIM) [28, 29] is applied to obtain the spatial domain half-space Green's functions in closed forms. The coupled PMCHW-CFIE is solved by BORMoM. A BOR object can be generated by rotating a generating arc about the axis of symmetry. We can take advantage of the rotational symmetry, and expand the currents on the BOR in Fourier series in azimuth φ. For this reason BOR simulations are often referred to as 2.5-D problems and can be solved efficiently with reduced memory and computation over their 3-D counterparts. Furthermore, with the aid of the Bohren decomposition scheme, the fields in chiral media can be decomposed into left- and right-handed Beltrami fields, which individually satisfy the Maxwell equations responding to two respective isotropic mediums characterized by equivalent isotropic parameters [5]. Once two uncoupled Beltrami fields are obtained by separately applying the surface equivalence principle to two equivalent isotropic mediums, the fields for chiral media can be obtained by a linear combination of the Beltrami fields.

The goal of this paper is to achieve accurate and fast analysis of the electromagnetic scattering by a conducting BOR coated with chiral media located above a lossy half-space. In Section 2, the theory and formulation for chiral coated conducting BOR above a half space is presented. Numerical examples are given to demonstrate the accuracy and efficiency of the proposed method in Section 3. Section 4 gives some conclusions. Throughout this paper, all fields and currents are considered to be time-harmonic with the time dependence of suppressed.

2. FORMULATION AND THEORY

2.1. PMCHW-CFIE Formulation

The configuration of an arbitrarily shaped BOR conducting body coated with chiral media in half-space is shown in Figure 1. The chiral media is characterized by (ε_c, μ_c, ξ), where ξ is chirality parameter. The dielectric parameters of half-space are (ε_{gr}, μ_{gr}) and (ε_0, μ_0) are the dielectric parameters of free-space. As shown in Figure 1, the dielectric surface is S_1, and the metallic surface is S_2. The composite structure is illuminated by an incident plane wave (E^{inc}, H^{inc}). By invoking the equivalence principle, the problem can be cast into an exterior and interior equivalent problem. By enforcing boundary conditions for the tangential electric and magnetic filed components on the BOR surface S_1 and S_2, one obtains coupled integral equations for the electric and magnetic surface currents, $\mathbf{J}_1$, $\mathbf{J}_2$ and $\mathbf{M}_1$, respectively. These integral equations can be put in a mixed potential form

$$\begin{aligned}
\text{On } S_1: \quad & \mathbf{E}^{ext}(\mathbf{J}_1,\mathbf{M}_1)|_{\tan} + \mathbf{E}_1^{int}(\mathbf{J}_1,\mathbf{M}_1)\big|_{\tan} + \mathbf{E}_2^{int}(\mathbf{J}_2)|_{\tan} \\
&= -\left(\mathbf{E}^{inc} + \mathbf{E}^{ref}\right)|_{\tan} \qquad (1) \\
& \mathbf{H}^{ext}(\mathbf{J}_1,\mathbf{M}_1)|_{\tan} + \mathbf{H}_1^{int}(\mathbf{J}_1,\mathbf{M}_1)\big|_{\tan} + \mathbf{H}_2^{int}(\mathbf{J}_2)|_{\tan} \\
&= -\left(\mathbf{H}^{inc} + \mathbf{H}^{ref}\right)|_{\tan} \qquad (2) \\
\text{On } S_2: \quad & \mathbf{E}_1^{int}(\mathbf{J}_1,\mathbf{M}_1)\big|_{\tan} + \mathbf{E}_2^{int}(\mathbf{J}_2)|_{\tan} = 0 \qquad (3) \\
& \mathbf{H}_1^{int}(\mathbf{J}_1,\mathbf{M}_1)\big|_{\tan} + \mathbf{H}_2^{int}(\mathbf{J}_2)|_{\tan} = -\mathbf{J}_2/2 \qquad (4)
\end{aligned}$$

where the subscript "tan" refers to vector components tangential to S_1 and S_2. $\mathbf{E}^{ext}(\mathbf{J}_1,\mathbf{M}_1)$ and $\mathbf{H}^{ext}(\mathbf{J}_1,\mathbf{M}_1)$represent the electric and magnetic fields radiated by the equivalent surface currents $\mathbf{J}_1$ and $\boldsymbol{M}_1$ in the upper half space environment, respectively. $\mathbf{E}_1^{int}(\mathbf{J}_1,\mathbf{M}_1)$ and $\mathbf{H}_1^{int}(\mathbf{J}_1,\mathbf{M}_1)$ denote the electric and magnetic fields radiated by equivalent surface currents $\mathbf{J}_1$ and $\mathbf{M}_1$ in the unbounded homogeneous chiral medium $(\varepsilon_c,\mu_c,\xi)$, respectively. $\mathbf{E}_2^{int}(\mathbf{J}_2)$ and $\mathbf{H}_2^{int}(\mathbf{J}_2)$ represent the electric fields radiated by the equivalent surface currents $\mathbf{J}_2$ in the unbounded homogeneous chiral medium $(\varepsilon_c,\mu_c,\xi)$. Note that the total incident field includes the incident field (E^{inc}, H^{inc}) and the reflected field (E^{ref}, H^{ref}) in the presence of the half-space.

The constitutive relationships for the homogeneous chiral medium $(\varepsilon_c,\mu_c,\xi)$ can be written as:

$$\mathbf{D} = \varepsilon_c\mathbf{E} - j\xi\mathbf{H} \qquad \mathbf{B} = \mu_c\mathbf{H} + j\xi\mathbf{E} \qquad (5)$$

It is well known that each of electromagnetic fields $\mathbf{E}$ and $\mathbf{H}$ in a homogeneous chiral medium can be decomposed into two waves,

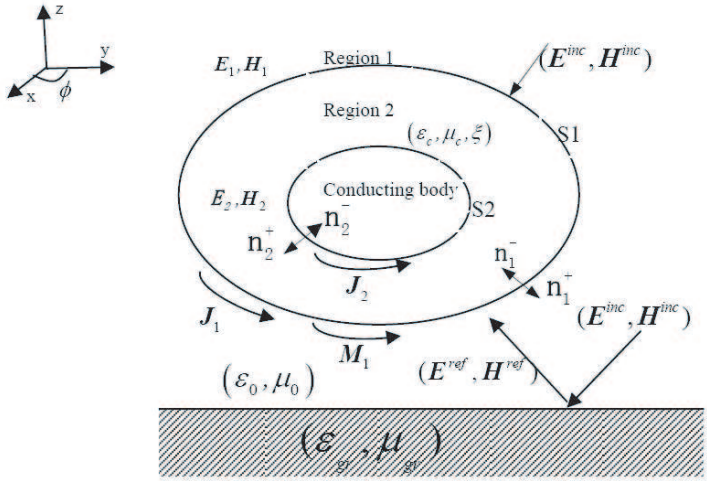

Figure 1. An arbitrarily conducting BOR coated with chiral media object located above half-space.

namely, the right-handed Beltrami fields ($\mathbf{E}_+$, $\mathbf{H}_+$) and left-handed Beltrami fields ($\mathbf{E}_-$, $\mathbf{H}_-$) [5]:

$$\mathbf{E} = \mathbf{E}_- + \mathbf{E}_+ \qquad \mathbf{H} = \mathbf{H}_- + \mathbf{H}_+ \tag{6}$$

where $\mathbf{E}_\pm = (1/2)(\mathbf{E} \mp j\eta_2\mathbf{H})$, $\mathbf{H}_\pm = (1/2)[\mathbf{H} \pm (j/\eta_2)\mathbf{E}]$ and the intrin-sic impedance is $\eta_2 = \sqrt{\mu_c/\varepsilon_c}$. The right- and left-handed Beltrami fields $\mathbf{E}_\pm$, $\mathbf{H}_\pm$ satisfies Maxwell's equations with $\varepsilon_\pm$, $\mu_\pm$ and the Beltrami current density $\mathbf{J}_\pm$, $\mathbf{M}_\pm$, where $\mathbf{J}_\pm = 1/2(\mathbf{J} \mp j/\eta_2\mathbf{M})$, $\mathbf{M}_\pm = 1/2(\mathbf{M} \mp j\eta_2\mathbf{J})$, $\varepsilon_\pm = \varepsilon_c \pm \xi/\eta_2$ and $\mu_\pm = \mu_c \pm \xi\eta_2$. Finally, the wavenumbers associated with the circularly polarized plane-wave fields are given by $k_\pm = \omega\sqrt{\mu_\pm\varepsilon_\pm} = \omega\sqrt{\mu_c\varepsilon_c}(1 \pm \xi_r)$, where $\xi_r = \xi/\sqrt{\varepsilon_c\mu_c}$ is the relative chirality. The interior equivalent fields are radiated by the equivalent surface currents $\mathbf{J}_1$, $\mathbf{J}_2$ and $\mathbf{M}_1$. It can be represented in terms of the mixed potential form:

$$\begin{aligned}\mathbf{E}_1^{int}(\mathbf{J}_1, \mathbf{M}_1) = \frac{1}{2}\{&[-L_+(\mathbf{J}_1) - K_+(\mathbf{M}_1)] + [-L_-(\mathbf{J}_1) - K_-(\mathbf{M}_1)] \\ &- j[-L_+(\mathbf{M}_1) + \eta_2 K_+(\mathbf{J}_1)] \\ &+ j[-L_-(\mathbf{M}_1) + \eta_2 K_-(\mathbf{J}_1)]\}\end{aligned} \tag{7}$$

$$\begin{aligned}\mathbf{H}_1^{int}(\mathbf{J}_1, \mathbf{M}_1) = \frac{1}{2}\{&[K_+(\mathbf{J}_1) - 1/\eta_2 L_+(\mathbf{M}_1)] + [K_-(\mathbf{J}_1) - 1/\eta_2 L_-(\mathbf{M}_1)] \\ &+ j/\eta_2[-L_+(\mathbf{J}_1) - K_+(\mathbf{M}_1)] \\ &- j/\eta_2[-L_-(\mathbf{J}_1) - K_-(\mathbf{M}_1)]\}\end{aligned} \tag{8}$$

$$\mathbf{E}_2^{int}(\mathbf{J}_2) = -\frac{1}{2}\left\{-L_+(\mathbf{J}_2) - L_-(\mathbf{J}_2) - j\eta_2\left[K_+(\mathbf{J}_2) - K_-(\mathbf{J}_2)\right]\right\} \quad (9)$$

$$\mathbf{H}_2^{int}(\mathbf{J}_2) = -\frac{1}{2}\left\{\left[K_+(\mathbf{J}_2) + K_-(\mathbf{J}_2)\right] - j/\eta_2\left[L_+(\mathbf{J}_2) - L_-(\mathbf{J}_2)\right]\right\} \quad (10)$$

where

$$K_\pm(\boldsymbol{\chi}) = \nabla \times \int_{S'} G_\pm\left(\mathbf{r}, \mathbf{r}'\right) \boldsymbol{\chi}\left(\mathbf{r}'\right) dS' \quad (11)$$

$$L_\pm(\boldsymbol{\chi}) = j\omega\mu_\pm \int_{S'} G_\pm\left(\mathbf{r}, \mathbf{r}'\right) \boldsymbol{\chi}\left(\mathbf{r}'\right) dS' - \frac{\nabla}{jw\varepsilon_\pm} \int_{S'} G_\pm\left(\mathbf{r}, \mathbf{r}'\right) \nabla \cdot \boldsymbol{\chi}\left(\mathbf{r}'\right) dS' \quad (12)$$

With $\mathbf{G}_\pm(\mathbf{r}, \mathbf{r}') = e^{-j\mathrm{K}_\pm|r-r'|}/(4\pi|\mathbf{r} - \mathbf{r}'|)$, $\mathbf{r}$ and $\mathbf{r}'$ denote the observation and sources points, respectively.

The exterior equivalent fields produced by the equivalent surface currents $\mathbf{J}_1$ and $\mathbf{M}_1$ in the upper half-space are given in terms of the mixed potential form, as follows:

$$\mathbf{E}^{ext}(\mathbf{J}_1, \mathbf{M}_1) = -L_h^e(\mathbf{J}_1) - K_h^e(\mathbf{M}_1) \quad (13)$$

$$\mathbf{H}^{ext}(\mathbf{J}_1, \mathbf{M}_1) = -L_h^m(\mathbf{M}_1) - K_h^m(\mathbf{J}_1) \quad (14)$$

where

$$K_h^e(\mathbf{M}) = -\int_{S'} \bar{\bar{G}}^{EM}(\mathbf{r}, \mathbf{r}') \cdot \mathbf{M}(\mathbf{r}') dS' \quad (15)$$

$$K_h^m(\mathbf{J}) = -\int_{S'} \bar{\bar{G}}^{HJ}(\mathbf{r}, \mathbf{r}') \cdot \mathbf{J}(\mathbf{r}') dS' \quad (16)$$

$$L_h^m(\mathbf{M}) = j\omega\varepsilon_0 \int_{S'} \bar{\bar{K}}_F\left(\mathbf{r}, \mathbf{r}'\right) \cdot \mathbf{M}\left(\mathbf{r}'\right) dS' - \frac{\nabla}{jw\mu_0} \int_{S'} K_{\phi m}\left(\mathbf{r}, \mathbf{r}'\right) \nabla \cdot \mathbf{M}\left(\mathbf{r}'\right) dS' \quad (17)$$

$$L_h^e(\mathbf{J}) = j\omega\mu_0 \int_{S'} \bar{\bar{K}}_A\left(\mathbf{r}, \mathbf{r}'\right) \cdot \mathbf{J}\left(\mathbf{r}'\right) dS' - \frac{\nabla}{jw\varepsilon_0} \int_{S'} K_{\phi e}\left(\mathbf{r}, \mathbf{r}'\right) \nabla \cdot \mathbf{J}\left(\mathbf{r}'\right) dS' \quad (18)$$

Details on the dyadic Green's function $\bar{\bar{K}}_A$, $\bar{\bar{K}}_F$, $\bar{\bar{G}}^{EM}$, $\bar{\bar{G}}^{HJ}$ and on the scalar Green's function $K_{\phi e}$, $K_{\phi m}$ can be found in [30]. According to "formulation C" in [30], the dyadic kernel functions $\bar{\bar{K}}_{A,F}(\mathbf{r}, \mathbf{r}')$ and dyadic Green's functions $\bar{\bar{G}}^{HJ,EM}(\mathbf{r}, \mathbf{r}')$ are written as:

$$\begin{aligned}\bar{\bar{K}}_{A,F} &= (\mathbf{xx}+\mathbf{yy})\, K_{A,F}^{\mathbf{xx}} + \mathbf{xz}K_{A,F}^{\mathbf{xz}} + \mathbf{yz}K_{A,F}^{\mathbf{yz}} + \mathbf{zx}K_{A,F}^{\mathbf{zx}} \\ &\quad + \mathbf{zy}K_{A,F}^{\mathbf{zy}} + \mathbf{zz}K_{A,F}^{\mathbf{zz}} \qquad (19)\\ \bar{\bar{G}}^{EM} &= G_{xx}^{EM}(\mathbf{xx}+\mathbf{yy}) + G_{xy}^{EM}\mathbf{xy} + G_{xz}^{EM}\mathbf{xz} + G_{yx}^{EM}\mathbf{yx} + G_{yz}^{EM}\mathbf{yz} \\ &\quad + G_{zx}^{EM}\mathbf{zx} + G_{zy}^{EM}\mathbf{zy} \qquad (20)\\ \bar{\bar{G}}^{HJ} &= G_{xx}^{HJ}(\mathbf{xx}+\mathbf{yy}) + G_{xy}^{HJ}\mathbf{xy} + G_{xz}^{HJ}\mathbf{xz} + G_{yx}^{HJ}\mathbf{yx} + G_{yz}^{HJ}\mathbf{yz} \\ &\quad + G_{zx}^{HJ}\mathbf{zx} + G_{zy}^{HJ}\mathbf{zy} \qquad (21)\end{aligned}$$

In general, the spatial domain Green's functions are expressed in terms of Sommerfeld integrals. Due to the highly oscillatory nature of the integrand, numerical integration is very time consuming. In this paper, a two-level Generalized Pencil of Function (GPOF) method is utilized to realize DCIM [29]. Then, the spatial domain Green's functions can be obtained in closed forms from their spectral-domain counterparts via the Sommerfeld identity.

To express (19)–(21) in a form suitable for the BOR problem, we utilize the transformations as shown in Figure 2:

$$\hat{n} = \cos v \cos\phi\hat{x} + \cos v \sin\phi\hat{y} - \sin v\hat{z} \qquad (22)$$

$$\hat{\phi} = -\sin\phi\hat{x} + \cos\phi\hat{y} \qquad (23)$$

$$\hat{t} = \cos\phi \sin v\hat{x} + \sin\phi \sin v\hat{y} + \cos v\hat{z} \qquad (24)$$

where $\hat{t}$ is a unit vector along the generating arc, $\hat{\phi}$ is a unit vector in the azimuthal direction, $\hat{n}$ is a unit normal vector along the generating

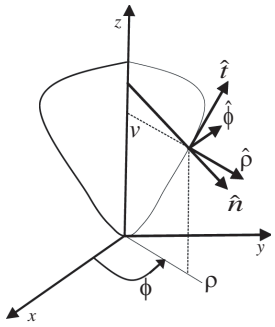

Figure 2. The transformation of coordinate system for the BOR.

arc and $\hat{\rho}$ is a unit radial vector along the generating arc. v is angle between the vectors $\hat{t}$ and $\hat{z}$, and v is positive when $\hat{t}$ points away from the **z** axis.

After substituting (6)–(9), (12) and (13) into (1)–(4), a set of coupled integral equations (PMCHW + CFIE) are obtained as follows:

$$\begin{aligned}
&1/2\left\{L_+\left(\mathbf{J}_1\right)+L_-\left(\mathbf{J}_1\right)+K_-\left(\mathbf{M}_1\right)+K_+\left(\mathbf{M}_1\right)+2L\left(\mathbf{J}_1\right)\right.\\
&+j\eta_2\left[K_+\left(\mathbf{J}_1\right)-K_-\left(\mathbf{J}_1\right)\right]+2K\left(\mathbf{M}_1\right)-j\left[L_+\left(\mathbf{M}_1\right)-L_-\left(\mathbf{M}_1\right)\right]\\
&\left.-L_-\left(\mathbf{J}_2\right)-L_+\left(\mathbf{J}_2\right)-j\eta_2\left[K_+\left(\mathbf{J}_1\right)-K_-\left(\mathbf{J}_1\right)\right]\right\}|_{\tan}=\mathbf{E}^{inc}|_{\tan} \quad (25)\\
&1/2\left\{j/\eta_2\left[L_+\left(\mathbf{J}_1\right)-L_-\left(\mathbf{J}_1\right)\right]-K_+\left(\mathbf{J}_1\right)-K_-\left(\mathbf{J}_1\right)\right.\\
&+j/\eta_2\left[K_+\left(\mathbf{M}_1\right)-K_-\left(\mathbf{M}_1\right)\right]-2K\left(\mathbf{J}_1\right)+2/\eta_1 L\left(\mathbf{M}_1\right)\\
&+1/\eta_2\left[L_+\left(\mathbf{M}_1\right)+L_-\left(\mathbf{M}_1\right)\right]+K_+\left(\mathbf{J}_2\right)+K_-\left(\mathbf{J}_2\right)\\
&\left.-j/\eta_2\left[L_+\left(\mathbf{J}_2\right)-L_-\left(\mathbf{J}_2\right)\right]\right\}|_{\tan}=\mathbf{H}^{inc}|_{\tan} \quad (26)\\
&\alpha/2\left\{L_+\left(\mathbf{J}_1\right)+L_-\left(\mathbf{J}_1\right)+j\eta_2\left[K_+\left(\mathbf{J}_1\right)-K_-\left(\mathbf{J}_1\right)\right]\right.\\
&+K_+\left(\mathbf{M}_1\right)+K_-\left(\mathbf{M}_1\right)-j\left[L_+\left(\mathbf{M}_1\right)-L_-\left(\mathbf{M}_1\right)\right]\\
&-L_+\left(\mathbf{J}_2\right)-L_-\left(\mathbf{J}_2\right)-j\eta_2\left[K_+\left(\mathbf{J}_2\right)-K_-\left(\mathbf{J}_2\right)\right]\}|_{\tan}\\
&+\eta_1\left(1-\alpha\right)/2\left\{\hat{n}_2\times\left[1/\eta_2\left(L_+\left(\mathbf{M}_1\right)+L_-\left(\mathbf{M}_1\right)\right)\right.\right.\\
&-K_+\left(\mathbf{J}_1\right)-K_-\left(\mathbf{J}_1\right)+j/\left(K_+\left(\mathbf{M}_1\right)-K_-\left(\mathbf{M}_1\right)\right)\\
&+j/\eta_2\left(L_+\left(\mathbf{J}_1\right)-L_-\left(\mathbf{J}_1\right)\right)+K_+\left(\mathbf{J}_2\right)+K_-\left(\mathbf{J}_2\right)\\
&\left.\left.-j/\eta_2\left(L_+\left(\mathbf{J}_2\right)-L_-\left(\mathbf{J}_2\right)\right)\right]-\mathbf{J}_2/2\right\}=0 \quad (27)
\end{aligned}$$

where $\eta_1=\sqrt{\mu_0/\varepsilon_0}$ and α is the combination parameter ranges from 0 to 1.

2.2. BORMoM Solution of PMCHW-CFIE

We expanded the unknowns $\mathbf{J}_1$, $\mathbf{J}_2$ and $\mathbf{M}_1$ in (25)–(27) with the rooftop triangular basis functions [31]. Due to the rotational symmetry of the BOR, the incident fields, surface currents and Green's functions are further expanded into discrete Fourier series along the azimuthal (ϕ or ϕ') direction. The currents are represented using rooftop triangular basis along the generating arc (coordinate t) and Fourier series expansion for the periodic azimuthal variation. The usage of the axisymmetric property of the BOR can convert an original electrically large BOR-problem into a series problem with small size of matrix equations, which can greatly reduce the computational cost. We call each small problem a Fourier mode of the original one. Using the Galerkin's method, a matrix equation for each Fourier mode n can be

obtained as:

$$\begin{bmatrix} [Z_{11n}^{JJ}] & [Z_{11n}^{JM}] & [Z_{12n}^{JJ}] \\ [Z_{11n}^{MJ}] & [Z_{11n}^{MM}] & [Z_{12n}^{MJ}] \\ [Z_{21n}^{JJ}] & [Z_{21n}^{JM}] & [Z_{22n}^{JJ}] \end{bmatrix} \begin{bmatrix} [I_{1n}] \\ [M_{1n}] \\ [I_{2n}] \end{bmatrix} = \begin{bmatrix} [V_n] \\ [U_n] \\ 0 \end{bmatrix} \tag{28}$$

Z is the impedance matrix for the nth Fourier mode. The superscripts J and M of Z_{12n}^{JM} denote the electric and magnetic currents, respectively. The subscript 1 of Z_{12n}^{JM} denotes equivalent currents along the exterior chiral surface of coated BOR, 2 denotes equivalent currents along the interior metal surface of coated BOR, n denotes the order of Fourier mode. I_{1n}, I_{2n} and M_{1n} are the column vectors containing the unknown coefficients of the electric and magnetic currents $\mathbf{J}_1$, $\mathbf{J}_2$ and $\mathbf{M}_1$ along the generating arc of chiral coated BOR, and V and U are the right-hand exciting vector depending on the Fourier series coefficients (nth mode) of the incident electric and magnetic fields tangential to the BOR. The detailed expressions of the impedance matrix blocks in (28) are defined as:

$$\begin{aligned} Z_{11}^{JJpq} = \Bigg\langle \vec{W}_{1ni}^{p} \quad & \frac{1}{2}\Big\{2L_h^e\left[\vec{J}_{1nj}^{q}\right] + L_+\left[\vec{J}_{1nj}^{q}\right] + L_-\left[\vec{J}_{1nj}^{q}\right] \\ & - j\eta_2\left(K_+\left[\vec{J}_{1nj}^{q}\right] - K_-\left[\vec{J}_{1nj}^{q}\right]\right)\Big\}\Bigg\rangle \end{aligned} \tag{29}$$

$$\begin{aligned} Z_{11}^{JMpq} = \Bigg\langle \vec{W}_{1ni}^{p} \quad & \frac{1}{2}\Big\{-2K_h^e\left[\vec{M}_{1nj}^{q}\right] - K_+\left[\vec{M}_{1nj}^{q}\right] - K_-\left[\vec{M}_{1nj}^{q}\right] \\ & - \frac{j}{\eta_2}\left(L_+\left[\vec{M}_{1nj}^{q}\right] - L_-\left[\vec{M}_{1nj}^{q}\right]\right)\Big\}\Bigg\rangle \end{aligned} \tag{30}$$

$$\begin{aligned} Z_{11}^{MJ\ pq} = \Bigg\langle \eta_1\vec{W}_{1ni}^{p} \quad & \frac{1}{2}\Big\{2K_h^m\left[\vec{J}_{1nj}^{q}\right] + K_+\left[\vec{J}_{1nj}^{q}\right] + K_-\left[\vec{J}_{1nj}^{q}\right] \\ & + \frac{j}{\eta_2}\left(L_+\left[\vec{J}_{1nj}^{q}\right] - L_-\left[\vec{J}_{1nj}^{q}\right]\right)\Big\}\Bigg\rangle \end{aligned} \tag{31}$$

$$\begin{aligned} Z_{11}^{MM\ pq} = \Bigg\langle \eta_1\vec{W}_{1ni}^{p}\frac{1}{2}\Big\{ & \frac{2}{\eta_1^2}L_h^m\left[\vec{M}_{1nj}^{q}\right] + \frac{1}{\eta_2^2}\left(L_+\left[\vec{M}_{1nj}^{q}\right] + L_-\left[\vec{M}_{1nj}^{q}\right]\right) \\ & - \frac{j}{\eta_2}\left(K_+\left[\vec{M}_{1nj}^{q}\right] - K_-\left[\vec{M}_{1nj}^{q}\right]\right)\Big\}\Bigg\rangle \end{aligned} \tag{32}$$

$$\begin{aligned} Z_{12}^{JJpq} = \Bigg\langle \vec{W}_{1ni}^{p} \quad & \frac{1}{2}\Big[-L_+\left[\vec{J}_{2nj}^{q}\right] - L_-\left[\vec{J}_{2nj}^{q}\right] \\ & + j\eta_2\left(K_+\left[\vec{J}_{2nj}^{q}\right] - K_-\left[\vec{J}_{2nj}^{q}\right]\right)\Big]\Bigg\rangle \end{aligned} \tag{33}$$

$$Z_{12}^{MJ\,pq} = \left\langle \eta_1 \vec{W}_{1ni}^{p} \quad \frac{1}{2}\left[-K_+\left[\vec{J}_{2nj}^{q}\right] - K_-\left[\vec{J}_{2nj}^{q}\right] - \frac{j}{\eta_2}\left(L_+\left[\vec{J}_{2nj}^{q}\right] - L_-\left[\vec{J}_{2nj}^{q}\right]\right)\right]\right\rangle \tag{34}$$

$$Z_{21}^{JJpq} = \left\langle \vec{W}_{2ni}^{p} \quad \begin{array}{l} \frac{\alpha}{2}\left\{L_+\left[\vec{J}_{1nj}^{q}\right] + L_-\left[\vec{J}_{1nj}^{q}\right] \right. \\ \eta_1\hat{n}\times\left(K_+\left[\vec{J}_{1nj}^{q}\right] + K_-\left[\vec{J}_{1nj}^{q}\right]\right. \\ \left. -j\eta_2\left(K_+\left[\vec{J}_{1nj}^{q}\right] - K_-\left[\vec{J}_{1nj}^{q}\right]\right)\right\} + \frac{1-\alpha}{2} \\ \left. +\frac{j}{\eta_2}L_+\left[\vec{J}_{1nj}^{q}\right] - \frac{j}{\eta_2}L_-\left[\vec{J}_{1nj}^{q}\right]\right) \end{array}\right\rangle \tag{35}$$

$$Z_{21}^{JMpq} = \left\langle \vec{W}_{2ni}^{p} \quad \begin{array}{l} \frac{\alpha}{2}\left\{-K_+\left[\vec{M}_{1nj}^{q}\right] - K_-\left[\vec{M}_{1nj}^{q}\right] \right. \\ \eta_1\hat{n}\times\left\{-\left(K_+\left[\vec{M}_{1nj}^{q}\right] - K_-\left[\vec{M}_{1nj}^{q}\right]\right)\right. \\ \left. -\frac{j}{\eta_2}\left(L_+\left[\vec{M}_{1nj}^{q}\right] - L_-\left[\vec{M}_{1nj}^{q}\right]\right)\right\} + \frac{1-\alpha}{2} \\ \left. +\frac{j}{\eta_2^2}\left(L_+\left[\vec{M}_{1nj}^{q}\right] + L_-\left[\vec{M}_{1nj}^{q}\right]\right)\right\} \end{array}\right\rangle \tag{36}$$

$$Z_{22}^{JJpq} = \left\langle \vec{W}_{2ni}^{p} \quad \begin{array}{l} \frac{\alpha}{2}\left[-L_+\left[\vec{J}_{2nj}^{q}\right] - L_-\left[\vec{J}_{2nj}^{q}\right] \right. \\ \eta_1\left\{-\hat{n}\times\left[K_+\left[\vec{J}_{2nj}^{q}\right] + K_-\left[\vec{J}_{2nj}^{q}\right]\right.\right. \\ \left. +j\eta_2\left(K_+\left[\vec{J}_{2nj}^{q}\right] - K_-\left[\vec{J}_{2nj}^{q}\right]\right)\right] + \frac{1-\alpha}{2} \\ \left.\left. +\frac{j}{\eta_2}\left(L_+\left[\vec{J}_{2nj}^{q}\right] - L_-\left[\vec{J}_{2nj}^{q}\right]\right)\right] - \frac{\vec{J}_{2nj}^{q}}{2}\right\} \end{array}\right\rangle \tag{37}$$

$$[\mathbf{I}_1]_n = \left[\left[I_{1n}^{t}\right]\left[I_{1n}^{\phi}\right]\right]^T \quad [\mathbf{M}_1]_n = \left[\left[M_{1n}^{t}\right]\left[M_{1n}^{\phi}\right]\right]^T \quad [\mathbf{I}_2]_n = \left[\left[I_{2n}^{t}\right]\left[I_{2n}^{\phi}\right]\right]^T \tag{38}$$

$$[V]_n = \left[\left[V_n^{t}\right]\left[V_n^{\phi}\right]\right]^T \quad [V_n^{p}]_i = \left\langle \vec{W}_{ni}^{\,p}, \vec{E}^{\,i} \right\rangle \tag{39}$$

$$[U]_n = \left[\left[U_n^{t}\right]\left[U_n^{\phi}\right]\right]^T \quad [U_n^{\alpha}]_i = \eta_1 \left\langle \vec{W}_{ni}^{\,\alpha}, \vec{H}^{\,i} \right\rangle \tag{40}$$

The superscript p and q denote $\mathbf{t}$ or ϕ direction. $\vec{W}_{1ni}^{p}$ and $\vec{W}_{2ni}^{p}$ denote the exterior and interior current testing rooftop basis functions, respectively. Thus, the linear system of equations in (28) can be

solved to obtain the unknown electric current and magnetic current coefficients. Finally, we can obtain the scattering characteristics of a conducting BOR coated with chiral media above a lossy half-space.

3. NUMERICAL RESULTS

In this section, we show some numerical results for electromagnetic characteristic of conducting BOR coated with chiral media above a lossy half-space that illustrate the accuracy and effectiveness of the proposed PMCHW-CFIE formulation solved by BORMoM. The PMCHW-CFIE linear systems based on the rooftop triangular basis functions are solved by the multifrontal direct solver [31]. All numerical experiments are performed on a Pentium 4 with 2.9 GHz CPU and 2 GB RAM in single precision.

The first example is a conducting sphere coated with chiral media in free space. The conducting sphere is coated by chiral media with inner radius of 0.9λ and outer radius of λ. The dielectric parameter of chiral media is chosen with $\varepsilon_{cr} = 2.667$, $\mu_{cr} = 1.333$ and $\xi_r = 0.5$. The frequency of incident electromagnetic wave is 300 MHz. The incident and scattered angle are $\theta_i = 0^\circ$, $\phi_i = 0^\circ$ and $\theta_s = 0$–180°, $\phi_s = 0^\circ$, respectively. Figure 3 gives the VV- and HH-polarized bistatic RCS for the above free-space chiral coated conducting sphere. It can be found that the results using the proposed BORMoM method are in good agreement with the results solved by GMRES method combined with fast multipole method (FMM) in [22]. Table 1 lists the comparison of number of unknowns, total computation time and RAM requirement between BORMoM and FMM method for the above chiral coated sphere in free space. The total computation time includes both the construction time of impedance matrix and the solution time of matrix equation. The chiral coated metallic sphere is discretized with triangular basis functions along the generating arc leading to 394 unknowns while the number of unknowns is 26799 in [22]. Compared with FMM, the BORMoM can save much RAM requirement by a factor of 5.9. It can be found that the BORMoM can also save much computation time by a factor of 14.7 than the FMM for this free-space example.

Next, we investigate electromagnetic scattering from a conducting BOR coated with chiral media above a lossy half-space. The second example is a conducting sphere coated with chiral media with inner radius of 0.25λ and outer radius of 0.3λ and is situated 0.4λ above half space characterized by $\varepsilon_{rg} = 5.0 - j0.2$ and $\mu_{gr} = 1.0$. The dielectric parameter of chiral media is chosen with $\varepsilon_{cr} = 3.0$, $\mu_{cr} = 1.0$, and $\xi_r = 0.3$. The target axis is orthogonal to the flat air-ground

interface. The frequency of incident electromagnetic wave is 300 MHz. The incident and scattered angle are $\theta_i = 0°$, $\phi_i = 0°$, $\theta_s = 0 - 90°$, $\phi_s = 0°$. The VV- and HH-polarized bi-static RCS for the half-space chiral coated conducting sphere are shown in Figure 4 The results obtained using the finite element-boundary integral method (FE-BI) are given in the same figures for comparison. Excellent agreements are observed between our BORMoM method and the FE-BI method. The chiral coated metallic sphere is discretized along the generating arc leading to 154 unknowns while the number of unknowns is 26799 in the FEBI method.

The last example is a conducting cylinder coated with chiral media above a lossy half-space. The coated conducting cylinder is with outer diameter of 0.6 m and inner diameter of 0.4 m, outer height of 0.5 m and inner height 0.3 m. It is located 0.3 m above a lossy half-

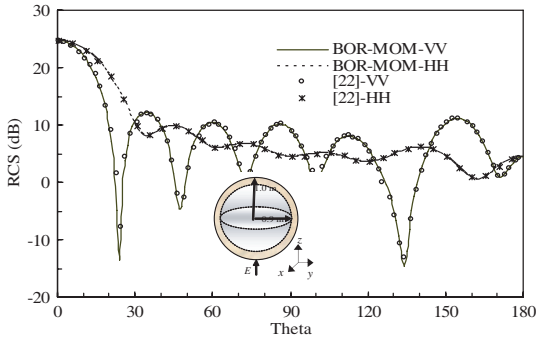

Figure 3. VV- and HH-polarized Bistatic RCS from a conducting sphere coated with chiral media in free space.

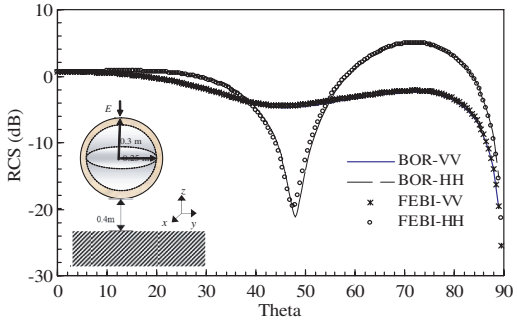

Figure 4. VV- and HH-polarized Bistatic RCS from a conducting sphere coated with chiral media located above a lossy half-space.

space characterized by $\varepsilon_{rg} = 5.0 - j0.2$ and $\mu_{gr} = 1.0$. The target axis is orthogonal to the flat air-ground interface. The parameter of coated chiral media (ε_{cr}, μ_{cr}, ξ) is chosen with (4.0, 1.0, 0.1) and (4.0, 1.0, 0.5), respectively. The incident angle of Plane-wave is $\theta_i = 0°$, $\phi_i = 0°$ with frequency 300 MHz. The VV-polarized bistatic RCS for the half-space chiral coated conducting cylinder are shown in Figure 5. The results obtained by FE-BI method are also given for comparison. In the computation, the chiral coated metallic cylinder is discretized with triangular basis functions leading to 198 unknowns while the number of unknowns is 19368 in the FEBI method. It can be found that the BORMoM results agree well with the results in FE-BI.

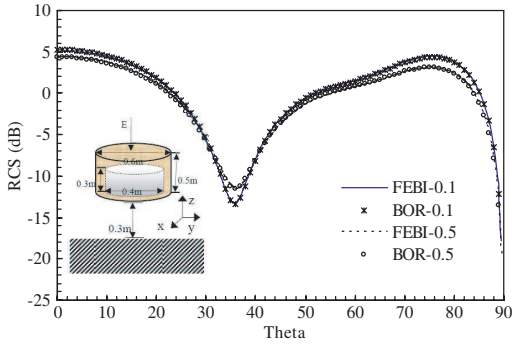

Figure 5. VV-polarized Bistatic RCS from a conducting cylinder coated with chiral media located above a lossy half-space.

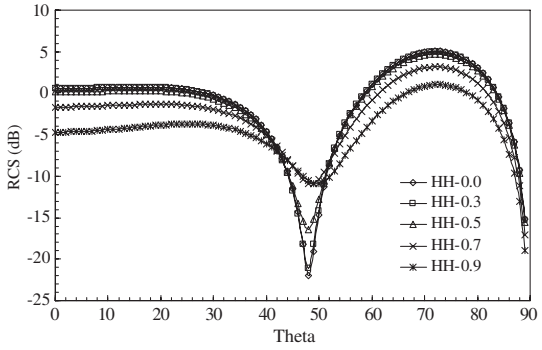

Figure 6. HH-polarized Bistatic RCS from a half-space conducting sphere coated with chiral media with $\xi_r = 0.0$, 0.3, 0.5, 0.7, 0.9.

Figures 6 and 7 show the VV- and HH-polarized bistatic RCS results for the above half-space coated conducting sphere example with chiral media $\xi_r = 0.3$, 0.5, 0.7, 0.9 and non-chiral media $\xi_r = 0.0$. The incident and scattered angle are $\theta_i = 0°$, $\phi_i = 0°$, $\theta_s = 0-90°$, $\phi_s = 0°$. As can be seen from the figures, there is an amplitude reduction of the RCS as compared to the non-chiral coated BOR. Furthermore, the amplitude reduction of the RCS is increase when the value of ξ_r increases from 0.0–0.9. It can be concluded that the chiral media has the properties of absorbing electromagnetic wave and can be used as a promising electromagnetic absorber material.

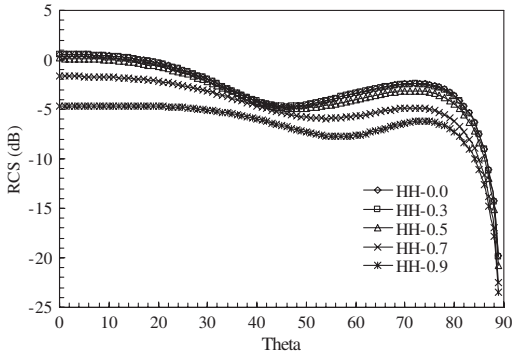

Figure 7. VV-polarized Bistatic RCS from a half-space conducting sphere coated with chiral media with $\xi_r = 0.0$, 0.3, 0.5, 0.7, 0.9.

Table 1. Comparison for the free-space conducting sphere coated with chiral media.

Method	Number of Unknowns	Total Computation Time	RAM
BORMoM	394	59.7 s	152 M
FMM in [22]	26799	881 s	893 M

Table 2. Comparison for the half-space conducting sphere coated with chiral media.

Method	Number of Unknowns	Total Computation Time	RAM
BORMoM	154	165.9 s	58 M
FE-BI	4780	11964.7 s	83 M

Table 3. Comparison for the half-space coated conducting cylinder with chiral media.

Method	Number of Unknowns	Total Computation Time	RAM
BORMoM	198	210.4 s	95 M
FE-BI	19368	24589.5 s	421 M

In order to further investigate the efficiency of the BORMoM method solving the coupled PMCHW-CFIE formulation for chiral coated BOR above a lossy half-space, Tables 2 and 3 list the comparison of number of unknowns, computation time and RAM requirement between BORMoM and FE-BI methods for the last two half-space examples. From Tables 2 and 3, it can be found that the BORMoM method can decrease the number of unknowns due to the usage of the axisymmetric property of the BOR. When compared with FE-BI method, the BORMoM decreases RAM requirement by a factor of 1.4 on the coated sphere example, 4.4 on the coated cylinder example. We further observed that the BORMoM method can greatly reduce the total computation time from Tables 2 and 3 because the BORMoM method can convert an original BOR-problem into a series problem with small size of matrix equations. When compared with FE-BI method, the BORMoM save time by a factor of 116.8 on the coated sphere example, 72.1 on the coated cylinder example.

4. CONCLUSION

In this paper, the coupled PMCHW-CFIE surface integral equation is extended for analyzing electromagnetic characteristic of conducting BOR coated with homogeneous chiral media above a lossy half-space. Due to the axisymmetric property of BOR, the BORMoM method is used to solve the linear system. The calculated results are validated with the FE-BI and FMM solutions to demonstrate the accuracy and efficiency of the proposed method. It can be found that the proposed BORMoM method is more efficient and can significantly reduce the overall computational cost.

ACKNOWLEDGMENT

The authors would like to thank the support of Natural Science Foundation of China under Contract Number 60701005, Open Research Program for State Key Laboratory of Millimeter Waves

under Contract Number K200808, Natural Science Foundation of Jangsu under Contact Number BK2009387 and the Research Fund for the Doctoral Program of Higher Education under Contract Number 20070288043.

REFERENCES

1. Dong, J. and C. Xu, "Characteristics of guided modes in planar chiral nihility meta-material waveguides," *Progress In Electromagnetics Research B*, Vol. 14, 107–126, 2009.
2. Hsu, H.-T. and C.-J. Wu, "Design rules for a Fabry-Perot narrow band transmission filter containing a metamaterial negative-index defect," *Progress In Electromagnetics Research Letters*, Vol. 9, 101–107, 2009.
3. Illahi, A. and Q. A. Naqvi, "Study of focusing of electromagnetic waves reflected by a PEMC backed chiral nihility reflector using Maslov's method," *Journal of Electromagnetic Waves and Applications*, Vol. 23, No. 7, 863–873, 2009.
4. Varadan, V. K., V. V. Varadan, and A. Lakhtakia, "On the possibility of designing anti-reflection coatings using chiral materials," *J. Wave-Mater. Interact.*, Vol. 2, No. 1, 71–81, 1987.
5. Bohren, C. F. and F. Craig, "Light scattering by an optically active sphere," *Chem. Phys. Lett.*, Vol. 29, No. 3, 458–462, Dec. 1974.
6. Bohren, C. F., "Scattering of electromagnetic waves by an optically active cylinder," *J. Colloid Interface, Sci.*, Vol. 66, No. 1, 105–109, Aug. 1978.
7. Chittayil, K. and A. Lakhtakia, "Electromagnetic scattering by a chiral cylinder immersed in another chiral medium," *Optik*, Vol. 89, 59–64, 1991.
8. Kluskens, M. S. and E. H. Newman, "Scattering by a chiral cylinder of arbitrary cross section," *IEEE Trans. Antennas Propag.*, Vol. 38, No. 9, 1448–1455, Sep. 1990.
9. Lakhtakia, A. and B. Shanker, "Beltrami fields within continuous source regions, volume integral equations, scattering algorithms, and the extended Maxwell-Garnett model," *Int. J. Appl. Electromagn. Mater.*, Vol. 4, 65–82, 1993.
10. Rojas, R. G., "Integral equations for EM scattering by homogeneous/inhomogeneous two-dimensional chiral bodies," *Inst. Elect. Eng. Microw., Antennas Propag.*, Vol. 141, No. 5, 385–392, May 1994.

11. Lakhtakia, A., V. K. Varadan, and V. V. Varadan, "Scattering and absorption characteristics of lossy dielectric, chiral, nonspherical objects," *Applied Optics*, Vol. 24, 4146–4154, 1985.
12. Lakhtakia, A., "The extended boundary condition method for scattering by a chiral scatterer in a chiral medium: Formulation and analysis," *Optik*, Vol. 86, 155–161, 1991.
13. Zhang, Y. J., A. Bauer, and E. P. Li, "T-matrix analysis of multiple scattering from parallel semi-circular channels filled with chiral media in a conducting plane," *Progress In Electromagnetics Research*, PIER 53, 299–318, 2009.
14. Worasawate, D., J. R. Mautz, and E. Arvas, "Electromagnetic scattering from an arbitrarily shaped three-dimensional homogeneous chiral body," *IEEE Trans. Antennas Propag.*, Vol. 51, No. 5, 1077–1084, 2003.
15. Yuceer, M., J. R. Mautz, and E. Arvas, "Moment of methods solution for the radar cross section of a chiral body of revolution," *IEEE Trans. Antennas Propag.*, Vol. 53, 1163–1167, 2005.
16. Dunn, E. A., J.-K. Byun, E. D. Branch, and J.-M. Jin, "Numerical simulation of BOR scattering and radiation using a higher order FEM," *IEEE Trans. Antennas Propag.*, Vol. 54, No. 3, 945–952, Mar. 2006.
17. Chen, J. and J. G. Wang, "A novel body-of-revolution finite-difference time-domain method with weakly conditional stability," *IEEE Microwave and Wireless Components Letters*, Vol. 18, No. 6, 377–399, Jun. 2008.
18. Demir, V., A. Z. Elsherbeni, and E. Arvas, "FDTD formulation for dispersive chiral media using the transform method," *IEEE Trans. Antennas Propag.*, Vol. 53, No. 10, 3374–3384, Oct. 2005.
19. Semichaevsky, A., A. Akyurtlu, D. Kern, D. H. Werner, and M. G. Bray, "Novel BI-FDTD approach for the analysis of chiral cylinders and spheres," *IEEE Trans. Antennas Propag.*, Vol. 54, No. 3, 925–932, Mar. 2006.
20. Wang, X. D., H. W. Douglas, L. W. Li, and Y. B. Gan, "Interaction of electromagnetic waves with 3-D arbitrarily shaped homogeneous chiral targets in the presence of a lossy half space," *IEEE Trans. Antennas Propag.*, Vol. 55, No. 12, 3647–3655, Dec. 2007.
21. Chen, R. S., Y. Q. Hu, Z. H. Fan, D. Z. Ding, D. X. Wang, and E. K. N. Yung, "An efficient surface integral equation solution to EM scattering by chiral objects above a lossy half space," *IEEE Trans. Antennas Propag.*, Vol. 57, No. 11, 3586–3593, 2009.

22. Wang, D. X., P. Y. Lau, E. K. N. Yung, and R. S. Chen, "Scattering by conducting bodies coated with bi-isotropic materials," *IEEE Trans. Antennas Propag.*, Vol. 55, No. 8, 2313–2319, Aug. 2007.
23. Ding, D.-Z., R.-S. Chen, and Z. H. Fan, "SSOR preconditioned inner-outer flexible GMRES method for MLFMM analysis of scattering of open objects," *Progress In Electromagnetics Research*, PIER 89, 339–357, 2009.
24. Ding, D. Z., R. S. Chen, Z. H. Fan, and P. L. Rui, "A novel hierarchical two-level spectral preconditioning technique for multilevel fast multipole analysis of electromagnetic wave scattering," *IEEE Trans. Antennas Propag.*, Vol. 56, No. 4, 1122–1132, Apr. 2008.
25. Umashankar, K., A. Taove, and S. M. Rao, "Electromagnetic scattering by arbitrarily shaped three-dimensional homogeneous lossy dielectric objects," *IEEE Trans. Antennas Propag.*, Vol. 34, No. 6, 758–766, 1986.
26. He, J. Q., T. J. Yu, N. Geng, and L. Carin, "Moment of methods analysis of electromagnetic scattering from a general three-dimensional dielectric target embedded in a multilayered medium," *Radio Sci.*, Vol. 35, 305–313, Mar.–Apr. 2000.
27. He, J. Q., A. Sullivan, and L. Carin, "Multilevel fast multipole algorithm for three-dimensional dielectric targets in the vicinity of a lossy half space," *Microw. Opt. Tech. Lett.*, Vol. 29, No. 2, 100–104, Apr. 2001.
28. Ding, D.-Z., R.-S. Chen, and Z. H. Fan, "Application of two-step spectral preconditioning technique for electromagnetic scattering in half-space," *Progress In Electromagnetics Research*, PIER 94, 383–402, 2009.
29. Aksun, M. I., "A robust approach for the derivation of closed-form Green's functions," *IEEE Trans. Microwave Theory and Techique*, Vol. 44, 651–658, May 1996.
30. Michalski, K. A. and D. Zheng, "Electromagnetic scattering and radiation by surfaces of arbitrary shape in layered media, part I: Theroy," *IEEE Trans. Antennas Propag.*, Vol. 38, 335–344, Mar. 1990.
31. Chen, R. S., L. Mo, and E. K. N. Yung, "Multifrontal method preconditioned GMRES-FFT algorithm for fast analysis of microstrip circuits," *International Journal for Computational and Mathematics in Electrical and Electronic Engineering*, Vol. 24, No. 1, 94–106, 2005.